Integrated design and operation of renewables-based fuels and power production networks

Qi Zhang[a], Mariano Martín[b,*], Ignacio E. Grossmann[a]

[a]*Center for Advanced Process Decision-making, Department of Chemical Engineering, Carnegie Mellon University, Pittsburgh, PA 15213, USA*
[b]*Department of Chemical Engineering, University of Salamanca, 37008 Salamanca, Spain*

Abstract

We assess the potential synergies of integrating renewables-based fuels and power production processes in one process network. In order to account for operational constraints as well as time-varying availability of renewable resources, such as wind and solar energy, we propose a multiscale mixed-integer linear programming model that combines the features of superstructure-based network synthesis and integrated production planning and scheduling. The model is applied to a case study for a particular region in Spain, where we analyze the feasibility of a renewables-based process network in terms of meeting given demands for gasoline, diesel, and electricity. The optimal and sometimes counterintuitive designs highlight the complex interactions and help identify bottlenecks in such process networks. Moreover, we solve each case using the multiscale model as well as a commonly used aggregate model; the two models obtain remarkably different solutions. A systematic comparison of the design decisions reveals the clear advantage of the multiscale model, which obtains high-quality solutions that stand the test of re-evaluation using a detailed model, whereas the aggregate model proposes network configurations that could in reality only satisfy small portions of the given diesel and electricity demands.

Keywords: Renewable energy, power production, biofuels production, integrated design and operation, process network

1. Introduction

In the light of increasing energy demand and climate change, many countries have intensified their efforts in shifting from fossil to renewable energy sources, of which the

*Corresponding author
Email address: mariano.m3@usal.es (Mariano Martín)

most commonly used ones are hydropower, wind, solar, and biomass. While the relatively high cost of existing biomass-to-energy conversion technologies has prohibited their widespread deployment at industrial scale, the main challenges for wind and solar power are their location- and time-dependent availability and the difficulty of storing electricity.

In the chemical industry, synergies between various processes are exploited by constructing and operating large integrated chemical complexes (Marechal and Kalitventzeff, 2003; Wassick, 2009; Varbanov and Klemeš, 2011). Similar approaches have been proposed to design sustainable energy systems. Yuan and Chen (2012) review optimal process synthesis approaches for biorenewable conversion, polygeneration, and carbon capture, and propose the integration of various energy conversion processes. Martín and Grossmann (2013) present an overview of systematic synthesis methods for sustainable biorefineries, while Yue et al. (2014) extend the scope to the design of bioenergy supply chains. In the area of power systems engineering, the design of wind- and solar-based power systems has been a major topic in recent years (Heide et al., 2010; Halamay et al., 2011; Sharifzadeh et al., 2017). Due to the intermittent nature of these renewable energy sources, their integration into the power grid significantly increases the complexity of classical optimal power flow (Dommel and Tinney, 1968) and unit commitment (Padhy, 2004) problems.

When it comes to the design of purely renewables-based energy systems, most existing works focus either on the production of fuels or on the generation of power. Recently, however, Martín and coworkers have systematically optimized various ways of integrating renewables-based power generation with the production of chemicals (Davis and Martín, 2014; Martín and Davis, 2016; Martín, 2016b,a; Martín and Grossmann, 2017a). In their latest work, Martín and Grossmann (2017b) consider the synthesis of process networks consisting of renewables-based energy conversion processes for both fuels and power production. The proposed multiperiod problem, in which each period represents one month of the year, is solved to determine the optimal selection of technologies in different regions of Spain. The results show that considerable synergies can be achieved, e.g. by storing electric energy in the form of chemicals that can be used to produce fuels.

Although the model proposed by Martín and Grossmann (2017b) helps identifying opportunities in such integrated process networks, it cannot consider effects at the operational level, which may have a significant impact on the design of the processes. For instance, intraday changes in wind velocity, solar incidence, and power demand are not captured; also, limitations with regard to process dynamics are not taken into account. The insufficient consideration of process operations can lead to designs that are

inadequately sized, resulting in infeasible or suboptimal operation.

As highlighted in a recent comprehensive review by Zhang and Grossmann (2016), considering process dynamics is particularly important in industrial demand side management, where power-intensive processes adapt their operation to changes in electricity price and take advantage of new demand response opportunities. Here, operational constraints have to be considered at the same level of granularity as the changes in the electricity market, which usually results in scheduling problems accounting for operational decisions at the hourly level. However, for design and long-term strategic problems, simply applying a detailed scheduling model to the entire time horizon (usually at least one year long) will inevitably lead to computational intractability; hence, multiscale models have been proposed in order to maintain the tractability of such problems.

Mitra et al. (2014) solve a capacity planning problem considering hourly changes in electricity price. In the proposed multiscale time representation, each year is divided into four seasons, and each season is represented by one week, which is repeated cyclically and characterized by a typical electricity price profile that reflects the price's seasonal behavior. With the proposed model, constraints on operational transitions can be formulated; however, the strictly cyclic schedules do not allow inventory to be carried over from one season to the next. Greater flexibility in inventory handling is achieved in the model proposed by Samsatli and Samsatli (2015), who focus on the modeling of transportation and storage operations in a supply chain setting, but do not model process dynamics as accurately as Mitra et al. (2014). Lara et al. (2017) solve a multiscale power network design problem by integrating a unit commitment formulation; however, the unit commitment problem does not take into account the times required for startup and shutdown, which are often significant in chemical plants. Zhang et al. (2017) apply two different time grids for modeling production and distribution operations in supply chains with power-intensive production facilities. Dowling et al. (2017) present a multiscale optimization framework for evaluating revenue opportunities provided by different layers of deregulated electricity markets for individual participants, and focus in particular on the real-time market. The model that comes closest to what we require in this work is the one proposed by Zhang et al. (2018), which considers process networks, allows restrictions on transitions between operating points, and accounts for inventory carried over across seasons. By applying the proposed mixed-integer linear programming (MILP) formulation, Zhang et al. (2018) solve a multistage long-term electricity procurement problem under demand uncertainty.

The objective of this work is to optimize the design of process networks for fuels and power production that solely make use of renewable (or quasi-renewable) energy sources. In order to appropriately do so, we combine a superstructure-based network

synthesis model and an integrated planning and scheduling model in a multiscale framework, which considers a planning horizon of one year and incorporates operational decisions at the hourly level.

The remainder of this paper is organized as follows. In Section 2, we present the problem statement including a detailed description of the superstructure network considered in this work. The integrated multiscale model is developed in Section 3. By applying the proposed model, we design a fuels and power production network for Almería, a province situated in the southeast of Spain. The results of this case study are presented and discussed in Section 5. Finally, in Section 6, we close with a brief summary and concluding remarks.

2. Problem statement

We consider the superstructure network proposed by Martín and Grossmann (2017b), as shown in Figure 1. The given network consists of two types of nodes: process nodes and resource nodes. Each process converts a specific set of input resources into its output resources. Process and resource nodes are connected by arcs, which depict the directions of the material or energy flows. The superstructure represents a superset of the set of feasible process networks, which can be generated by selecting different combinations of process and resource nodes.

Table 1 lists the processes and their corresponding input and output resources. As input resources for the whole energy system (indicated by hatched resource nodes), we only consider renewable energy sources, such as wind, solar, hydro, biomass, and waste. Lignocellulosic biomass can be biochemically (P21) or thermally (P1) processed to bioethanol or syngas, respectively. Syngas can be further processed into hydrogen and CO_2 through a water-gas shift reaction (P3) or directly used to produce power (P2), hydrogen (P19), ethanol (P19), methanol (P20), Fischer-Tropsch liquids (P22), or simply thermal energy (P16). Wind is used for power generation (P4), and solar energy can be captured using photovoltaic (PV) panels (P7) or mirrors using concentrated solar power (CSP) technologies (P8a). Hydropower offers a way to store power by elevating water and maintaining its potential energy (P14), which is converted into kinetic energy (P13) when power needs to be generated. Furthermore, waste can be used to produce biogas, with which power can then be generated using a gas and a steam turbine (P15). Through electrolysis (P5), power can be used to produce hydrogen, which in turn can serve as input resource for methanol (P6) or methane (P17) production. While methane can further be used in a gas turbine (P18), methanol is processed in the transesterification of oil (P12). The oil can be extracted from algae (P11), which require sun light and CO_2 to grow. Finally, cooling processes are also included in the network in order

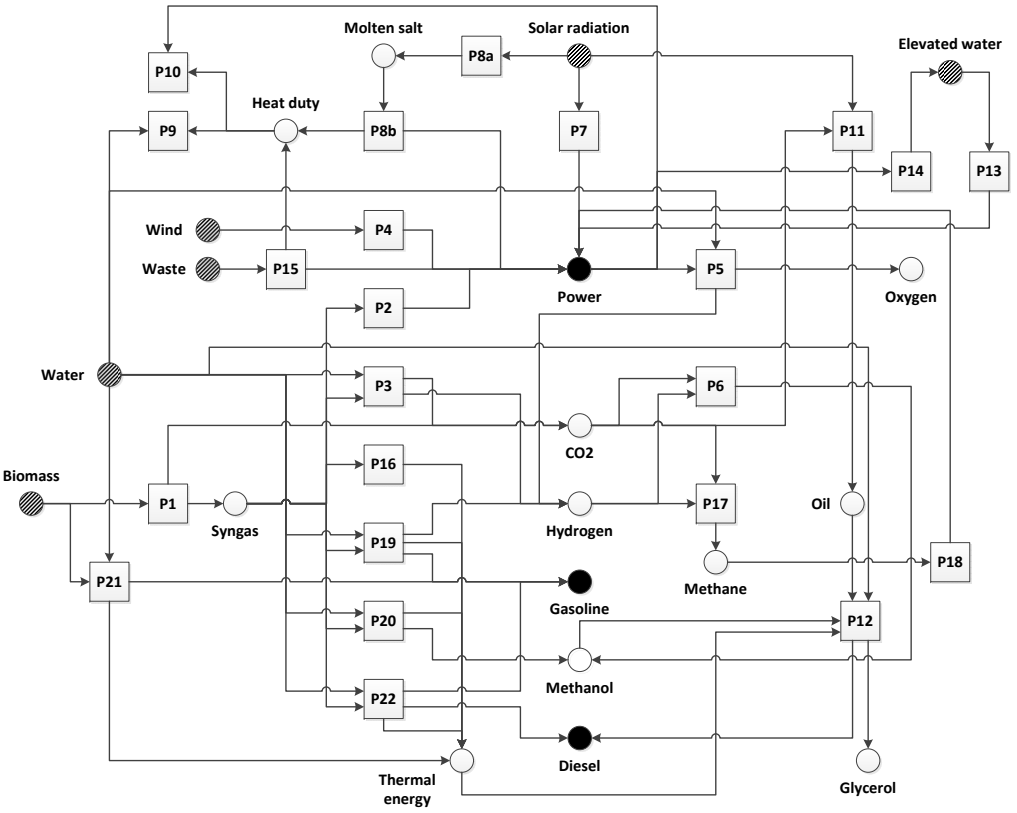

Figure 1: Superstructure network for renewables-based fuels and power production. The network representation consists of process nodes (rectangles) and resources nodes (circles) connected by arcs, which depict the directions of the material and energy flows.

to remove the heat generated by some processes (P9, P10). Note that some resources, such as the air feed for P9 and P10, are not included in the network because they are not relevant for the optimization.

Consider a geographical region for which we have information on water and biomass availability, wind velocity, and solar incidence. The objective is to design a process network to be built at this location in order to satisfy given demands for power, gasoline, and diesel, at minimum capital and operating costs. Operation over the course of one year is considered as this time horizon is deemed to be sufficiently representative for a system exhibiting strong seasonal behaviors. The optimal sizing of the plants should be ensured by accounting for detailed scheduling decisions; hence, for every time period of the planning horizon, we determine:

- the mode of operation for each process,

Table 1: Overview of processes and the corresponding input and output resources.

Name	Description	Input Resources	Output Resources
P1	Gasification	Biomass	Syngas
P2	Gas turbine	Syngas	Power
P3	Water-gas shift reaction	Water, syngas	Hydrogen, CO_2
P4	Wind turbine	Wind	Power
P5	Electrolysis	Water, power	Hydrogen, oxygen
P6	Methanol production	Hydrogen, CO_2	Methanol
P7	Photovoltaics	Solar radiation	Power
P8a	Concentrated solar power (charging)	Solar radiation	Energy stored in molten salt
P8b	Concentrated solar power (discharging)	Energy stored in molten salt	Power, heat duty
P9	Cooling tower	Water, heat duty	
P10	Air cooling	Power, heat duty	
P11	Algae-based oil production	Solar radiation, CO_2	Oil
P12	Transesterification of oil	Oil, water, methanol, thermal energy	Diesel substitute, glycerol
P13	Hydropower (discharging)	Elevated water	Power
P14	Hydropower (charging)	Power	Elevated water
P15	Enzymatic digestion, power generation	Waste	Power, heat duty
P16	Furnace	Syngas	Thermal energy
P17	Methane production	Hydrogen, CO_2	Methane
P18	Gas turbine	Methane	Power
P19	Thermochemical bioethanol production	Syngas, water	Hydrogen, gasoline substitute, thermal energy
P20	Biomethanol production	Syngas, water	Methanol, thermal energy
P21	Biochemical bioethanol production	Biomass, water	Gasoline substitute, thermal energy
P22	Fischer-Tropsch process	Syngas, water	Gasoline substitute, diesel substitute, thermal energy

- the processing rate in each process,
- the material and energy flows in the process network,

- the amount of input resources required,
- the amount of intermediate and final products stored.

3. Model formulation

In the following, we present the proposed MILP model for this integrated design, planning, and scheduling problem. The underlying scheduling formulation is based on the mode-based discrete-time model proposed by Zhang et al. (2016); for further details, we refer the reader to that reference. Note that unless specified otherwise, continuous variables in this model are constrained to be nonnegative. A list of indices, sets, parameters, and variables is given in the Nomenclature section.

3.1. Multiscale time representation

In this problem, we have to consider a variety of time-dependent effects, which do not necessarily follow the same diurnal and seasonal behavior. For instance, the availability of water for hydropower mainly depends on the weather, whereas fuels demand tends to peak during national holiday seasons. Wind velocity and solar incidence change significantly over the course of a day. The same is true for power demand; in addition, power demand profiles exhibit different behaviors for different days of the week. In order to capture the response of the processes to these time-varying conditions, we have to adequately account for constraints on process dynamics and inventory, while maintaining a manageable model size.

In the proposed multiscale time representation, which is illustrated in Figure 2, the planning horizon (in this case a year) is divided into seasons, denoted by index h. Note that the seasons can, but do not have to correspond to the four seasons of a year (spring, summer, autumn, and winter). The set of seasons, H, is specified according to the reoccurring patterns that characterize the different time-varying parameters; hence, the seasons can also have different lengths. Each season h consists of a representative set of time periods, $\overline{T}_h$, which starts at time point 0. Time periods considered before time 0 are used to track past mode transitions. All time periods are of equal length, Δt (e.g. an hour).

In each season h, a cyclic schedule over the given set of time periods is applied n_h times. Note that although the time periods before time 0 for one season overlap with the last time periods of the previous season, only the discrete mode transition decisions are identical in these time periods. More importantly, despite the cyclic schedule, the inventory level at the end of a season is allowed to be different from the inventory level at the beginning of the season; the accumulated inventory is carried over to the next season.

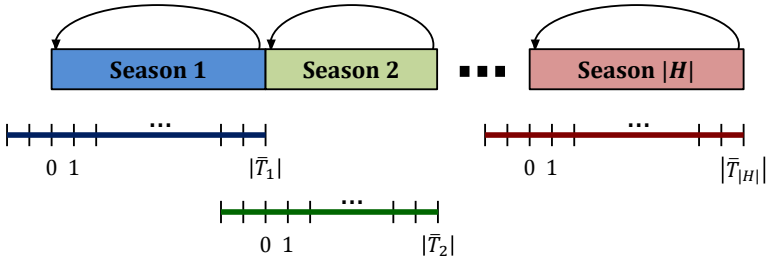

Figure 2: Multiscale time representation, which divides the planning horizon into seasons, with each season represented by a specific set of time periods.

3.2. Network design constraints

Derived from the superstructure shown in Figure 1, the network design is given by the selected nodes, which represent production processes and storage facilities, and their capacities. We define the binary variable x_i that equals 1 if process i is selected. Similarly, the binary variable $\bar{x}_j$ equals 1 if a storage facility is built for resource j. The following constraints limit the capacities that can be realized:

$$C_i \le C_i^{\max} x_i \quad \forall\, i \tag{1a}$$

$$\overline{C}_j \le \overline{C}_j^{\max} \bar{x}_j \quad \forall\, j \tag{1b}$$

$$x_i \in \{0,1\} \quad \forall\, i \tag{1c}$$

$$\bar{x}_j \in \{0,1\} \quad \forall\, j \tag{1d}$$

where C_i is the production capacity for process i, and $\overline{C}_j$ is the storage capacity for resource j. The maximum allowed capacities are denoted by $C_i^{\max}$ and $\overline{C}_j^{\max}$. Note that $\overline{C}_j^{\max} = 0$ for nonstorable resources such as power.

3.3. Mode-based operation

In this model, we assume that each process can operate in different operating modes, which represent operating states such as *off*, *on*, *startup*, and *shutdown*. Each operating mode is characterized by a given production range. We introduce the binary variable y_{imht}, which equals 1 if process i operates in mode m in time period t of season h. The mode-based operation is captured by the following constraints:

$$\sum_{m \in M_i} y_{imht} = x_i \quad \forall\, i, h, t \in \overline{T}_h \tag{2a}$$

$$P_{iht} = \sum_{m \in M_i} \overline{P}_{imht} \quad \forall\, i, h, t \in \overline{T}_h \tag{2b}$$

$$\widetilde{C}_{im}^{\min} y_{imht} \le \overline{P}_{imht} \le \widetilde{C}_{im}^{\max} y_{imht} \quad \forall\, i, m \in M_i, h, t \in \overline{T}_h \tag{2c}$$

$$y_{imht} \in \{0,1\} \quad \forall\, i,\, m \in M_i,\, h,\, t \in \overline{T}_h \tag{2d}$$

where M_i is the set of operating modes for process i. Eq. (2a) states that if process i is selected, it has to operate in one mode in every time period. In Eq. (2b), the amount of reference resource produced or consumed in mode m is denoted by $\overline{P}_{imht}$, which is zero if mode m is not selected. The production range for each mode is specified in Eq. (2c).

The main advantage of the mode-based formulation is that it allows us to formulate constraints on transitions, which occur when the system changes from one operating point to another. For changes between operating points in the same operating mode, a bound on the rate of change, $\bar{\Delta}_{im}^{\max}$, can be set as follows:

$$\begin{aligned} -\bar{\Delta}_{im}^{\max} - \overline{M}(2 - y_{imht} - y_{imh,t-1}) \le \overline{P}_{imht} - \overline{P}_{imh,t-1} \\ \le \bar{\Delta}_{im}^{\max} + \overline{M}(2 - y_{imht} - y_{imh,t-1}) \quad \forall\, i,\, m \in M_i,\, h,\, t \in \overline{T}_h \end{aligned} \tag{3}$$

where $\overline{M}$ is a big-M parameter of appropriate size.

Additional constraints have to be imposed on transitions between different operating modes, which is achieved by enforcing constraints (4)–(6). The binary variable $z_{imm'ht}$ equals 1 if and only if process i switches from mode m to mode m' at time t, which is stated in the following equations:

$$\sum_{m' \in \overline{TR}_{im}} z_{im'mh,t-1} - \sum_{m' \in \widehat{TR}_{im}} z_{imm'h,t-1} = y_{imht} - y_{imh,t-1} \quad \forall\, i,\, m \in M_i,\, h,\, t \in \overline{T}_h \tag{4a}$$

$$z_{imm'ht} \in \{0,1\} \quad \forall\, i,\, (m,m') \in TR_i,\, h,\, t \in \overline{T}_h \tag{4b}$$

with TR_i being the set of all possible mode-to-mode transitions in process i, $\overline{TR}_{im} = \{m' : (m',m) \in TR_i\}$, and $\widehat{TR}_{im} = \{m' : (m,m') \in TR_i\}$.

The restriction that a plant has to remain in a certain mode for a minimum amount of time after a transition is stated as follows:

$$y_{im'ht} \ge \sum_{k=1}^{\theta_{imm'}} z_{imm'h,t-k} \quad \forall\, i,\, (m,m') \in TR_i,\, h,\, t \in \overline{T}_h \tag{5}$$

with $\theta_{imm'}$ being the minimum stay time in mode m' after switching to it from mode m.

For predefined sequences, each defined as a fixed chain of transitions from mode m to mode m' to mode m'', we can specify a fixed stay time in mode m' by imposing the

following constraint:

$$z_{imm'h,t-\bar{\theta}_{imm'm''}} = z_{im'm''ht} \quad \forall\, i, (m, m', m'') \in SQ_i,\, h,\, t \in \overline{T}_h \tag{6}$$

where SQ_i is the set of predefined sequences for process i and $\bar{\theta}_{imm'm''}$ is the fixed stay time in mode m' in the corresponding sequence.

3.4. Mass balance constraints

We assume that all processes are operated continuously. For some processes, e.g. algae-based oil production and biochemical bioethanol production, this assumption does not necessarily hold true; however, these plants usually have a large number of units (e.g. ponds and fermenters) such that they can be operated in an almost continuous fashion. The mass balance constraints can be stated as follows:

$$Q_{jht} = (1 - \epsilon_{jh}) Q_{jh,t-1} + \sum_i \sum_{m \in M_i} \rho_{imjh} \overline{P}_{imht} + B_{jht} - S_{jht} \quad \forall\, j,\, h,\, t \in \overline{T}_h \tag{7a}$$

$$P_{iht} \le \eta_{iht} C_i \quad \forall\, i,\, h,\, t \in \overline{T}_h \tag{7b}$$

$$Q_{jht} \le \overline{C}_j \quad \forall\, j,\, h,\, t \in \overline{T}_h \tag{7c}$$

$$B_{jht} \le B_{jht}^{\max} \quad \forall\, j,\, h,\, t \in \overline{T}_h \tag{7d}$$

$$S_{jht} \ge D_{jht} \quad \forall\, j \in \bar{J},\, h,\, t \in \overline{T}_h \tag{7e}$$

$$S_{jht} = 0 \quad \forall\, j \in \hat{J},\, h,\, t \in \overline{T}_h \tag{7f}$$

where Q_{jht} is the inventory level for resource j at time period t of season h, P_{iht} is the amount of reference resource produced or consumed in process i, B_{jht} is the amount of resource j consumed by the process network, and S_{jht} is the amount of resource j discharged from the network. Eq. (7a) is the inventory balance. The parameter ϵ_{jh} accounts for loss from storage. The conversion factor ρ_{imjh} is given with respect to the reference resource; depending on the sign of ρ_{imjh}, resource j is either produced or consumed by process i in mode m.

Eq. (7b) limits P_{iht} by the built capacity C_i. The parameter η_{iht} accounts for time-varying production capacities, such as those of power generation facilities that make use of wind and solar energy. Eq. (7c) limits Q_{jht} by the built storage capacity $\overline{C}_j$. As stated in Eq. (7d), the amount of resource j consumed by the process network is bounded by $B_{jht}^{\max}$. In this case, $B_{jht}^{\max}$ is only nonzero for the resources indicated by hatched resource nodes in Figure 1. The set of resources, for which demand is given, is denoted by $\bar{J}$ (indicated by filled resource nodes in Figure 1). According to Eq. (7e), the demand D_{jht} is satisfied by the discharged amount. Eq. (7f) sets S_{jht} to zero for $j \in \hat{J}$, the set of resources that must not be discharged, e.g. heat duty.

3.5. Continuity equations

Continuity equations are required at the boundaries of each season in order to maintain mass balance and feasible transitions. The cyclic schedules are enforced by applying the following constraints:

$$y_{imh,0} = y_{imh,|\overline{T}_h|} \quad \forall\, i,\, m \in M_i,\, h \tag{8a}$$

$$z_{imm'ht} = z_{imm'h,t+|\overline{T}_h|} \quad \forall\, i,\, (m,m') \in TR_i,\, h,\, -\theta_i^{\max} + 1 \le t \le -1 \tag{8b}$$

which state that the system at the end of each representative time horizon has to be in the same mode as at the beginning of the same time horizon, while having a cyclic mode transition schedule.

Similarly, the state in which the system is at the end of one season has to match the beginning of the next season:

$$y_{imh,|\overline{T}_h|} = y_{im,h+1,0} \quad \forall\, i,\, m \in M_i,\, h \in H \setminus \{|H|\} \tag{9a}$$

$$z_{imm'h,t+|\overline{T}_h|} = z_{imm',h+1,t} \quad \forall\, i,\, (m,m') \in TR_i,\, h \in H \setminus \{|H|\},\, -\theta_i^{\max} + 1 \le t \le -1. \tag{9b}$$

Despite the cyclic schedule, we allow inventory to be accumulated over the course of a season and carried over to the next by applying the following constraints:

$$\overline{Q}_{jh} = Q_{jh,|\overline{T}_h|} - Q_{jh,0} \quad \forall\, j,\, h \tag{10a}$$

$$Q_{jh,0} + n_h\, \overline{Q}_{jh} = Q_{j,h+1,0} \quad \forall\, j,\, h \in H \setminus \{|H|\} \tag{10b}$$

$$Q_{j,|H|,0} + n_{|H|}\, \overline{Q}_{j,|H|} \ge Q_{j,1,0} \quad \forall\, j \tag{10c}$$

where $\overline{Q}_{jh}$ denotes the excess inventory, which according to Eq. (10a) is defined as the difference between the inventory levels at the end and at the beginning of a representative time horizon. As indicated in Eq. (10b), since the cyclic schedule in season h is repeated n_h times, $n_h\, \overline{Q}_{jh}$ is accumulated over the course of the season and carried over to the next. Eq. (10c) is a terminal constraint, stating that the final inventory level should not be below the initial inventory level. Note that $\overline{Q}_{jh}$ is the only continuous variable in this model that can also take negative values.

3.6. Objective function

The annualized capital costs for the various processes, denoted by V_i, are approximated by piecewise-linear functions of the plant capacities, which are formulated as

follows:

$$C_i = \sum_{l \in L_i} \left[\lambda_{il} (\widehat{C}_{i,l-1} - \widehat{C}_{il}) + \widehat{C}_{il}\, w_{il} \right] \quad \forall\, i \tag{11a}$$

$$V_i = \sum_{l \in L_i} \left[\lambda_{il} (\widehat{V}_{i,l-1} - \widehat{V}_{il}) + \widehat{V}_{il}\, w_{il} \right] \quad \forall\, i \tag{11b}$$

$$\lambda_{il} \leq w_{il} \quad \forall\, i,\, l \in L_i \tag{11c}$$

$$\sum_{l \in L_i} w_{il} = x_i \quad \forall\, i \tag{11d}$$

$$w_{il} \in \{0, 1\} \quad \forall\, i,\, l \in L_i \tag{11e}$$

with L_i being the set of pieces for the piecewise-linear approximation for process i. Each line segment l is defined by its two end points, each given by a capacity-cost pair, i.e. $(\widehat{C}_{i,l-1}, \widehat{V}_{i,l-1})$ and $(\widehat{C}_{il}, \widehat{V}_{il})$. The binary variable w_{il} equals 1 if the chosen capacity C_i is in the range of line segment l. The exact position on the line is then given by λ_{il}, which takes a value between 0 and 1.

Assuming linear capital costs for storage facilities, the total annualized capital cost, CC, is given by

$$CC = \sum_i V_i + \sum_j \left(\alpha_j\, \bar{x}_j + \beta_j\, \overline{C}_j \right). \tag{12}$$

The total operating cost, OC, is given by

$$OC = \sum_h \sum_{t \in \overline{T}_h} n_h \left[\sum_i \sum_{m \in M_i} \left(\delta_{imh}\, y_{imht} + \gamma_{imh}\, \overline{P}_{imht} \right) + \sum_j \phi_{jh}\, B_{jht} + \sum_j \psi_{jh}\, S_{jht} \right] \tag{13}$$

where we assume mode-dependent linear operating cost functions. The last two terms constitute the costs for purchasing and discharging resources; in our particular case, we assume that only biomass needs to be purchased, and only discharging CO_2 incurs a cost in form of a carbon tax. Note that the cost coefficients can vary across seasons.

The objective is to minimize the total cost, TC, which consists of the capital and operating costs:

$$TC = CC + OC. \tag{14}$$

This finally results in the following optimization problem, which we will refer to as the

multiscale problem (MP):

$$\begin{aligned} \min \quad & TC \\ \text{s.t.} \quad & \text{Eqs. (1)–(14).} \end{aligned} \tag{MP}$$

4. Detailed and aggregate models

In order to properly assess the design decisions obtained from (MP), we have to apply them to the detailed problem that does not make the simplifying assumption of cyclic schedules based on representative data for each season, but treats each time period of the year individually. The model for this detailed problem, which we denote by (DP), can be obtained from adapting (MP) by performing the following steps:

1. Replace season-dependent time set $\overline{T}_h$ by $\widehat{T}_h = \{1, 2, \ldots, n_h|\overline{T}_h|\}$.
2. Replace η_{iht}, $B^{\max}_{jht}$, and D_{jht} by $\hat{\eta}_{iht}$, $\widehat{B}^{\max}_{jht}$, and $\widehat{D}_{jht}$, respectively, as the latter are the actual data from which the season-representative parameters in (MP) are generated.
3. Remove Eqs. (8).
4. Replace Eqs. (10) by $Q_{j,|H|,|\widehat{T}_h|} \geq Q_{j,1,0} \quad \forall\, j$.
5. Replace n_h in Eq. (13) by 1.

The main purpose of this work is the assessment of the potential benefit of applying a multiscale model to this network design problem instead of an aggregate model that does not take constraints at the operational level into account. We derive the aggregate model by removing the operational constraints from (DP) and aggregating the remaining constraints and corresponding variables for each season h over the time set

$\widehat{T}_h$, which results in the following formulation:

$$
\begin{aligned}
\min \quad & CC + \widehat{OC} \\
\text{s.t.} \quad & \text{Eqs. (1), (11), (12)} \\
& \widehat{Q}_{jh} = \widehat{Q}_{j,h-1} + \sum_i \hat{\rho}_{ijh}\, \widehat{P}_{ih} + \widehat{B}_{jh} - \widehat{S}_{jh} \quad \forall\, j,\, h \\
& \widehat{P}_{ih} \le \tilde{\eta}_{ih}\, C_i \quad \forall\, i,\, h \\
& \widehat{Q}_{jh} \le \overline{C}_j \quad \forall\, j,\, h \\
& \widehat{B}_{jh} \le \widetilde{B}^{\max}_{jh} \quad \forall\, j,\, h \\
& \widehat{S}_{jh} \ge \widetilde{D}_{jh} \quad \forall\, j \in \bar{J},\, h \\
& \widehat{S}_{jh} = 0 \quad \forall\, j \in \hat{J},\, h \\
& \widehat{Q}_{j,|H|} \ge \widehat{Q}_{j,0} \quad \forall\, j \\
& \widehat{OC} = \sum_h \left[\sum_i \left(|\widehat{T}_h|\, \hat{\delta}_{ih}\, x_i + \hat{\gamma}_{ih}\, \widehat{P}_{ih} \right) + \sum_j \left(\phi_{jh}\, \widehat{B}_{jh} + \psi_{jh}\, \widehat{S}_{jh} \right) \right]
\end{aligned}
\tag{AP}
$$

where $\widehat{Q}_{jh} = Q_{jh,|\widehat{T}_h|}$, the aggregated variables are $\widehat{P}_{ih} := \sum_{t \in \widehat{T}_h} P_{iht}$, $\widehat{B}_{jh} := \sum_{t \in \widehat{T}_h} B_{jht}$, and $\widehat{S}_{jh} := \sum_{t \in \widehat{T}_h} S_{jht}$, and the aggregated parameters are $\tilde{\eta}_{ih} = \sum_{t \in \widehat{T}_h} \hat{\eta}_{iht}$, $\widetilde{B}^{\max}_{jh} = \sum_{t \in \widehat{T}_h} \widehat{B}^{\max}_{jht}$, and $\widetilde{D}_{jh} = \sum_{t \in \widehat{T}_h} \widehat{D}_{jht}$. The coefficients $\hat{\rho}_{ijh}$, $\hat{\delta}_{ih}$, and $\hat{\gamma}_{ij}$ are chosen by assuming that process i is constantly operating in a specific mode. There is no loss term in the mass balance equation since ϵ_{jh} is assumed to be zero. Note that the aggregate model (AP) is very similar to the model applied by Martín and Grossmann (2017b) and is therefore well-suited for comparison purposes in our case study.

5. Results and discussion

We apply the proposed model to design a renewables-based process network for Almería, a province in the southeast of Spain. The goal is to demonstrate the advantage of the multiscale model over the aggregate model and to evaluate the amount of fuels and power demand that can be satisfied with a purely renewables-based system at this particular location. The planning horizon of one year is divided into four 13-week long seasons, each represented by one representative week with hourly time discretization.

5.1. Case study data

All process-related capacity, conversion, and cost data are adapted from Martín and Grossmann (2017b) and can be found in that reference. The minimum stay times related to mode transitions are based on computational experiments and practical considerations and can be found in the supplementary material.

This case study is based on resource availability and fuels and power demand data from 2016. Almería is considered one of the driest regions in Europe; hence, the available amounts of biomass and water are relatively small. However, there is abundant solar radiation and also, the average wind speed is fairly high as Almería has a coastline on the Mediterranean Sea. In 2016, the estimated total amounts of biomass (averaged from miscanthus, straw, and forest residues), waste (manure from cattle, pigs, and sheep), and water are 105 kt (Bioenarea, 2016; Edwards et al., 2006), 1310 kt (MAPAMA, 2016), and 16,071 kt (SAIH Hidrosur, 2017), respectively. The average wind speed at 80 m height is 4.7 m/s (CENER, 2017), and the average annual solar irradiance is 1804 kWh/m^2 (Datosclima.es, 2017). We assume that the availability of biomass and waste is evenly distributed over the course of the year. Amounts of available water, wind, and solar are given on an hourly basis and can be found in the supplementary material. We assume that 1 % of the amount of available water is readily available elevated water for hydropower.

The annual demands for gasoline, diesel, and electricity are, respectively, 49 kt, 427 kt (CORES, 2016), and 2863 GWh (Red Electrica de Espana, 2017). In this case study, the gasoline and diesel demands are given at the seasonal level, i.e. assuming constant demand over the course of each season, while the electricity demand is given at the hourly level. These data are as well provided in the supplementary material.

5.2. Computational considerations

All models were implemented in Julia with the JuMP package (Lubin, M., Dunning, 2015) and solved using CPLEX 12.7 on an Intel® Core™ i7-2600 machine at 3.40 GHz with 8 processors and 8 GB RAM. Table 2 shows the model sizes and solution times for (MP), (AP), and (DP). The multiscale model (MP) has more than 700,000 variables, among which more than half a million are binary variables, and almost half a million constraints. Yet the model is still relatively efficient; in all instances, it could be solved in less than five hours to 1% optimality gap. The aggregate model (AP) is several orders of magnitude smaller and therefore solves in less than a second. Because of its substantially larger size, the full-space detailed model (DP) could not be solved as the machine ran out of memory.

In order to compare the quality of the solutions obtained from (MP) and (DP), in each case, the design decisions are fixed in (DP), which is then solved in a rolling-horizon fashion. For this problem, we choose the prediction horizon to be four weeks and the implementation horizon to be one week long, i.e. while moving forward in time, a scheduling problem for the next four weeks is solved, but only the first week is implemented. We introduce slack variables for unmet demand in (DP) in order to guarantee

Table 2: Model sizes and solution times.

	(MP)	(AP)	(DP)
# of bin. variables	530,033	109	4,239,360
# of cont. variables	201,816	484	1,797,120
# of constraints	486,392	547	5,957,216
Solution time	< 5 h *	< 1 s	n/a

* solved to 1 % optimality gap

feasibility. After the full detailed problem is solved for a particular set of design decisions, we record the total operating cost and the actual satisfied demand.

5.3. Optimization results

We determine the optimal process network for Almería in three cases (Cases A, B, and C) that differ in demand and CO_2 and biomass availability. In each case, we set the demand of gasoline, diesel, and electricity close to what is maximum feasible. We solve all cases using (MP) and (AP) and compare the results by applying the obtained design decisions to (DP) as described in the previous section.

5.3.1. Case A: base case

For Case A, we set the demands for gasoline, diesel, and electricity to respectively 10 %, 5 %, and 60 % of the total amounts required in Almería. For ease of direct comparison, Figure 3 shows both the network design decisions obtained from (MP) and (AP). In the figure, network nodes highlighted in yellow are selected in the solution from (MP) whereas nodes highlighted in green are selected by (AP). Nodes selected by both (MP) and (AP) have a double yellow-green coloring. The numbers (red for (MP) and green for (AP)) indicate the production and storage capacities. Already at first glance, one can see that the two solutions are very different. Here, we make the following observations:

- (MP) suggests using more power generation technologies and building significantly more capacity for power generation than (AP). (AP) only generates solar power using CSP (P8) whereas (MP) also uses photovoltaics (P7). This is mainly due to the fact that unlike (AP), (MP) considers hourly changes in resource availability and hence suggests a design that can compensate for periods of low solar radiation.

- Water is a scarce resource in Almería, which is reflected in the solutions that suggest using air coolers (P10) instead of cooling towers (P9) for cooling. For the same reason, hydropower generation is not considered in the proposed designs.

- Solar radiation is very high in Almería while wind speed is relatively low, which makes solar power more cost-effective. As a result, neither of the two solutions selects power generation from wind.

- Power generation from waste (P15) is only used in the (MP) solution. The constant supply of waste helps mitigate the variability in power generation using solar energy. This need is not seen by (AP) as it assumes that solar radiation is available at constant rate in each season.

- In addition to the Fischer-Tropsch process (P22), both (MP) and (AP) also suggest using the algae-based oil production (P11) and the subsequent transesterification of oil (P12) to produce diesel. However, (MP) installs considerable storage capacities for CO_2, oil, and diesel in order to mitigate the impact of variable solar radiation, whereas (AP) only considers relatively moderate storage capacity for diesel since it assumes algae growth with constant average solar incidence.

- While (AP) suggests producing methanol from syngas and water (P20), (MP) synthesizes methanol from CO_2 and hydrogen (P6). The reason for this difference is that unlike (AP), (MP) sees the need for building CO_2 inventory during operation. Therefore, (MP) uses the water-gas shift reaction (P3) to produce more CO_2, and hydrogen as well. At that point, it becomes more economical to produce methanol through P6 than through P20.

- Power is not stored chemically in the form of methane due to the high cost of producing synthetic methane (P17) and because it would require CO_2 and hydrogen, which are needed for the production of diesel.

Table 3 compares the solutions obtained from (MP) and (AP) in terms of the actual satisfied demands, capital expenses, and operating expenses, evaluated by applying the design decisions to the detailed model (DP). One can see that 100 % of the specified gasoline demand is satisfied by both solutions. (MP) meets well above 90 % of the diesel and electricity demands, which, given the fluctuations in electricity demand and solar incidence, is acceptable for initial design purposes. (AP), however, only covers 81 % and 60 % of the diesel and electricity demands, respectively, which is attributed to the fact that (AP) disregards detailed operational decisions and hence cannot account for demand and resource variability.

Naturally, due to the significantly smaller number of processes built and lower demand satisfaction, the CAPEX and OPEX for the (AP) solution are considerably lower than the numbers obtained from the (MP) solution. In the case of (MP), the annualized

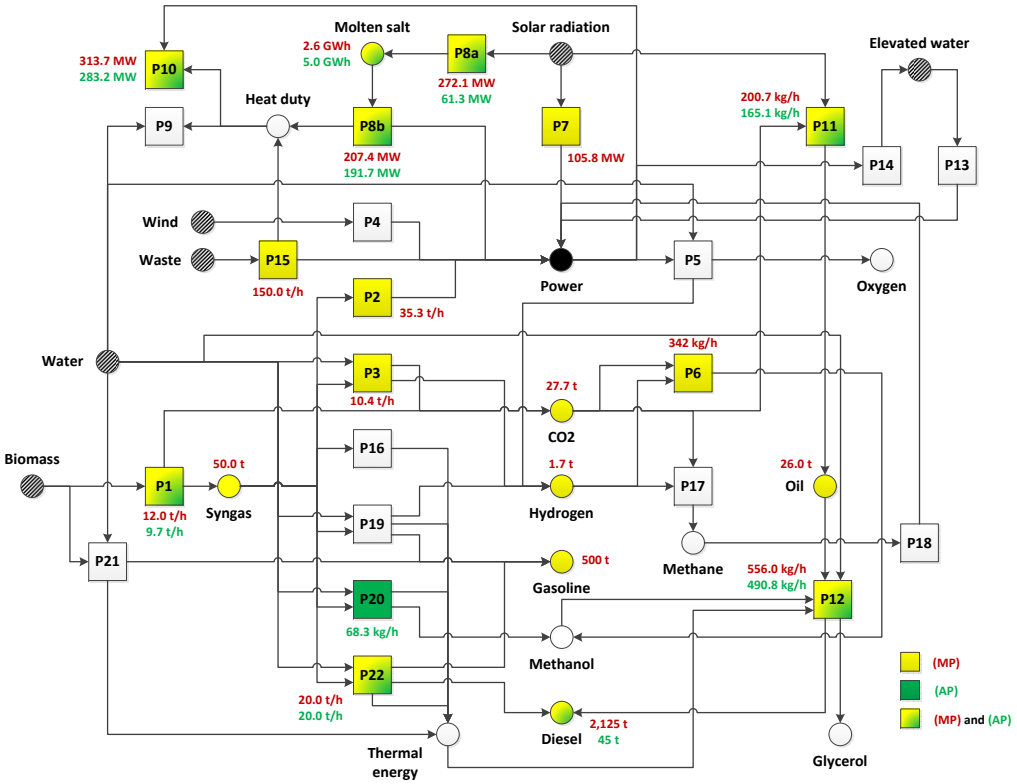

Figure 3: Process network designs proposed by (MP) and (AP) for Case A.

Table 3: Comparison between solutions obtained from (MP) and (DP) for Case A.

	Actual satisfied demand (%)			CAPEX (€M/yr)	OPEX (€M/yr)
	Gasoline	Diesel	Electricity		
(MP)	100	92	93	44.4	33.5
(AP)	100	81	60	14.1	15.1

CAPEX is €44.4 million, and the annual OPEX amounts to €33.5 million. The breakdown of the CAPEX into the selected processes is shown in Figure 4, which indicates that more than 3/4 of the total CAPEX is spent on solar power capacities (PV and CSP).

To show the decisions made at the operational level by (MP), we present the power generation schedule for the representative winter week in Figure 5. The plot shows the amount of electricity generated or consumed by each process (only P10 consumes electricity) as well as the inventory profile for molten salt. One can clearly see how the

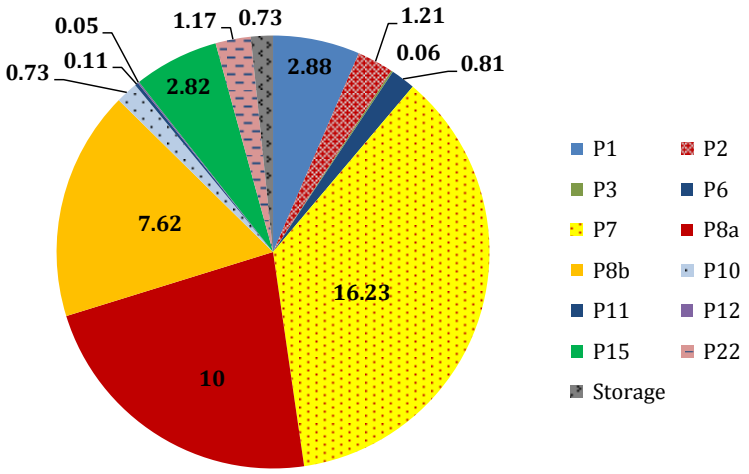

Figure 4: Breakdown of CAPEX proposed by (MP) for Case A (numbers given in €M).

solution benefits from the combination of PV and CSP plants, namely by generating electricity using PV panels during periods of high solar incidence while charging the CSP storage, and generating electricity using the CSP plant during periods of low solar incidence.

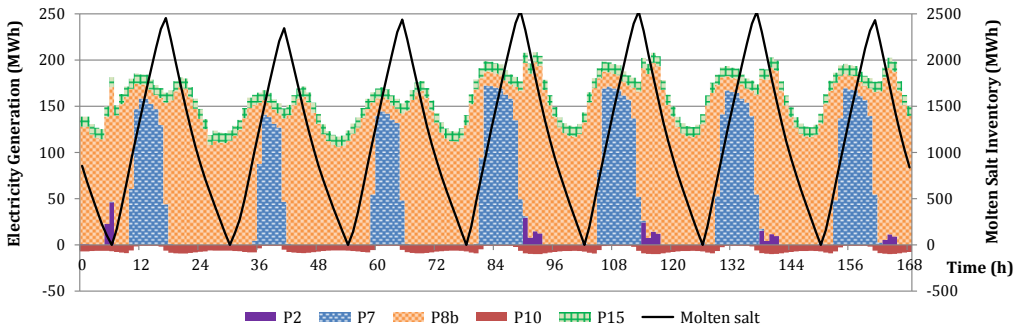

Figure 5: Power generation schedule for the representative winter week proposed by (MP) for Case A.

5.3.2. Case B: external CO_2 input

In Case A, one major bottleneck for biodiesel production is the availability of CO_2, which is needed as the carbon source for algae growth in P11. In Case A, CO_2 has to be entirely produced within the process network with no additional external input; however, in reality, there may be plenty of external CO_2 sources, e.g. conventional CO_2-emitting power plants and concrete production. By using CO_2 from such sources, we

would not only be able to increase biodiesel production, but would also reduce CO_2 emissions. Therefore, in Case B, we allow external CO_2 input and analyze its impact on the design decisions. Demands for gasoline, diesel, and electricity are set to respectively 10 %, 10 %, and 60 % of the total amounts required in Almería.

Figure 6 shows the network design decisions obtained from (MP) and (DP), and Table 4 shows the actual satisfied demands, capital expenses, and operating expenses. We first discuss the differences in the (MP) solution compared to Case A:

- Due to the increased availability of CO_2, sufficient amount of methanol can be produced using P6. As a result, the Fischer-Tropsch process (P22) is not selected anymore to meet diesel demand since it is significantly more expensive. The thermal energy required for P12, which is mainly produced by P22 in Case A, is now provided by the combustion of syngas (P16) and the thermochemical bioethanol production process (P19), which have been added to the network in Case B. P19 also produces hydrogen, hence reducing the need for expensive hydrogen storage.
- Compared to Case A, the production capacities of P11 and P12 have been significantly increased.
- The solution suggests installing large storage capacities for oil and methanol in order to deal with the variability in solar incidence that affects the algae-based oil production.
- Interestingly, both the CAPEX and the OPEX in Case B are lower than in Case A although more diesel is produced. Besides the cost savings achieved by excluding P22 from the process network, this result is mainly attributed to the substantial reduction in required PV capacity (from 105.8 to 62.7 MW). This is possible because of the increased power generation by P2 during operation, which is used to offset the reduced power generation from PV panels. This considerable increase in the capacity of using syngas for power generation is in turn made possible by the fact that diesel is now produced through P12 instead of P22 due to the higher availability of CO_2; otherwise, like in Case A, P22 would consume a large portion of the syngas.

Similar to Case A, there is also a stark difference between the network configurations proposed by (MP) and (AP) in Case B. As shown in Figure 6, unlike (MP), (AP) suggests using P20 and P21 to produce methanol and gasoline, respectively. However, like (MP), (AP) also only relies on P12 to produce diesel. Here, the most remarkable observation is that the actual diesel demand met by the (AP) solution is only 4 % (see Table 4). As the (AP) predicts full demand satisfaction, this discrepancy seems to be overly excessive at

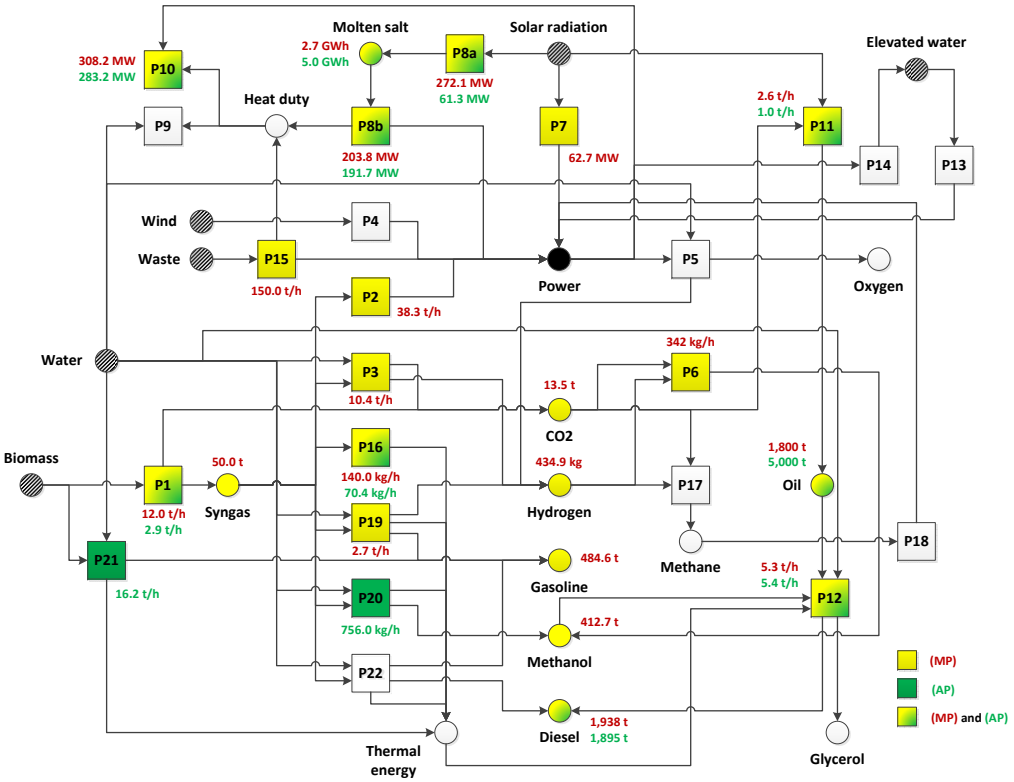

Figure 6: Process network designs proposed by (MP) and (AP) for Case B.

first; however, the explanation for this phenomenon becomes clear when we take a close look at the operational restrictions imposed by the proposed design. The major design flaw lies in the lack of methanol storage capacity. Since the aggregate model (AP) does not consider detailed operations, it assumes that the processes can operate at constant rate, in which case the production capacities would be just sufficient to satisfy the given demand. Yet in reality, due to the high variability in solar incidence, little amount of oil is produced during hours of low solar radiation, resulting in P20 not being able to utilize its full methanol production capacity without any methanol storage since P12 would not be able to process it without sufficient amount of oil. In addition, the (AP) solution provides misleading inventory information (at the seasonal level); as a result, when solving (DP) in a rolling-horizon fashion, oil inventory is not built to an extent that would allow full utilization of P20 and P12.

Table 4: Comparison between solutions obtained from (MP) and (DP) for Case B.

	Actual satisfied demand (%)			CAPEX (€M/yr)	OPEX (€M/yr)
	Gasoline	Diesel	Electricity		
(MP)	100	92	97	38.5	31.1
(AP)	100	4	59	20.8	6.1

5.3.3. Case C: increased biomass availability

The main limiting resource for such a renewables-based process network in Almería is biomass, which in turn is a result of the scarce water availability. Although it has not been demonstrated, desertification of the south of Spain has been related to climate change. In Case C, in addition to allowing external CO_2 input, we increase the availability of biomass by 100 %. Also, demands for gasoline, diesel, and electricity are increased to 20 %, 20 %, and 65 % of the total amounts required in Almería, respectively. The results are shown in Figure 7 and Table 5. In terms of the (MP) solution, the main differences to Case B are the following:

- Compared to Case B, a number of processes, in particular P1, P6, P7, P11, and P12, have increased significantly in size in Case C in order to meet the higher demands, naturally resulting in considerably higher CAPEX and OPEX.
- As P12 alone does not suffice to meet the demand anymore; hence, both P12 and P22 are used to produce diesel. The production of green gasoline and Fischer-Tropsch diesel results in P19 not being selected for the production of bioethanol. Furthermore, P3 and P16 are no longer used.
- In order to increase methanol production using P6, electrolysis (P5) is selected to produce more hydrogen and substantial storage capacities for hydrogen and CO_2 are added.
- Power generation from wind (P4) is now selected, mainly to provide the additional electricity required by the electrolyzers.

With regard to the selection of processes, the (AP) solution for Case C does not differ from the one for Case B; hence, it also exhibits similar shortcomings, including only actually meeting a tiny fraction of the diesel demand due to the lack of methanol storage.

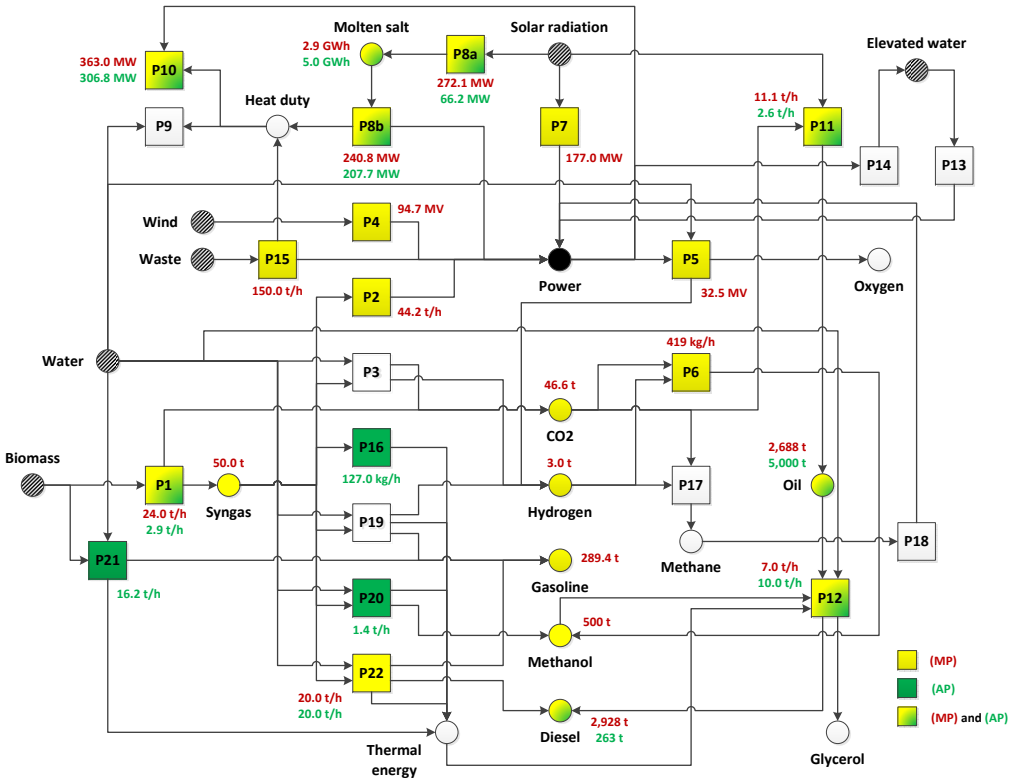

Figure 7: Process network designs proposed by (MP) and (AP) for Case C.

Table 5: Comparison between solutions obtained from (MP) and (DP) for Case C.

	Actual satisfied demand (%)			CAPEX (€M/yr)	OPEX (€M/yr)
	Gasoline	Diesel	Electricity		
(MP)	100	96	97	75.3	48.1
(AP)	100	0.3	57	29.3	7.0

6. Conclusions

In this work, we have developed a multiscale MILP model for the integrated optimal design and operation of renewables-based fuels and power production networks. The proposed model allows the selection of a feasible process network derived from a given superstructure network, while simultaneously optimizing detailed operational schedules for the selected processes. We have demonstrated the effectiveness of the proposed model by applying it to a case study for Almería, a province situated in the southeast of

Spain.

In the case study, we have emphasized the comparison between the design decisions obtained from the multiscale model and from a commonly used aggregate model. Each set of design decisions is evaluated by applying it to a detailed scheduling model for the entire one-year time horizon, which is solved in a rolling-horizon fashion. The results highlight the main take-away from this paper: When designing systems involving time-varying resources, e.g. wind and solar, proper design decisions can only be made if operational considerations are taken into account at the same time. While this was achieved by the proposed multiscale model, the aggregate model, which disregards operational constraints, obtained inadequate network designs that could only satisfy small portions of the given diesel and electricity demands.

In the particular case of Almería, the results show that about 10 % of gasoline, 5 % of diesel, and 60 % of electricity demand for the region can be met by an entirely renewables-based process network, which generates the vast majority of the electricity using solar power while making ample use of the storage capability of the CSP plant. The diesel demand that can be met increases to about 10 % if external CO_2 input is allowed, which significantly increases the network's capacity for algae-based diesel production. The main limiting factor for the process network turns out to be the availability of biomass.

Although the proposed model is general, the results are very specific to the geographical region to which is was applied. Future work will involve exploiting further synergies by simultaneously optimizing such process networks for multiple regions, and the development of solution algorithms for solving these large-scale problems more efficiently.

Nomenclature

Indices / sets

$h \in H$	seasons
$i \in I$	processes
$j \in J$	resources
$l \in L$	segments in piecewise-linear approximations
$m \in M$	operating modes
$t \in T$	time periods, $T = \{-\theta^{\max} + 1, -\theta^{\max} + 2, \ldots, 0, 1, \ldots, \lvert T \rvert\}$

Subsets

$\bar{J}$	resources with demand
$\hat{J}$	resources that must not be discharged
L_i	segments in piecewise-linear approximation for process i
M_i	operating modes in process i
SQ_i	predefined sequences of mode transitions in process i
$\overline{T}_h$	time periods in season h, $\overline{T}_h = \{1, 2, \ldots, \lvert\overline{T}_h\rvert\}$
TR_i	possible mode transitions in process i
$\overline{TR}_{im}$	modes from which mode m can be directly reached in process i
$\widehat{TR}_{im}$	modes which can be directly reached from mode m in process i

Parameters

$B^{\max}_{jht}$	maximum amount of resource j that can be consumed by the process network in time period t of season h
$C^{\max}_i$	maximum production capacity for process i
$\overline{C}^{\max}_j$	maximum storage capacity for resource j
$\widehat{C}_{il}$	production capacity for process i at right end point of segment l
$\widetilde{C}^{\max}_{im}$	maximum production amount in mode m of process i
$\widetilde{C}^{\min}_{im}$	minimum production amount in mode m of process i
D_{jht}	demand for resource j in time period t of season h
$\overline{M}$	big-M parameter in rate-of-change constraint
n_h	number of times the representative scheduling horizon of season h is repeated
$\widehat{V}_{il}$	capital cost for process i at right end point of segment l
α_j	fixed capital cost for storing resource j
β_j	unit capital cost for storing resource j
δ_{imh}	fixed cost for operating in mode m of process i in season h
Δt	length of one time period
$\bar{\Delta}^{\max}_{im}$	maximum rate of change
γ_{imh}	unit cost for operating in mode m of process i in season h
ϵ_{jh}	fractional loss from storing resource j in season h
η_{iht}	fractional availability of production capacity in process i in time period t of season h
	mode m of process i in season h
$\theta_{imm'}$	minimum stay time in mode m' of process i after switching from mode m to m'
$\bar{\theta}_{imm'm''}$	fixed stay time in mode m' of the predefined sequence (m, m', m'') in process i
$\theta^{\max}$	maximum minimum or predefined stay time in a mode
ρ_{imjh}	conversion factor for resource j with respect to the reference resource in
ϕ_{jh}	unit cost for purchasing resource j in season h
ψ_{jh}	unit cost for discharging resource j in season h

Unrestricted continuous variables

$\overline{Q}_{jh}$ excess inventory for resource j in season h

Nonnegative continuous variables

B_{jht}	amount of resource j consumed by the process network in time period t of season h
C_i	production capacity for process i
$\overline{C}_j$	storage capacity for resource j
CC	annualized capital cost
OC	annual operating cost
P_{iht}	amount of reference resource produced by process i in time period t of season h
$\overline{P}_{imht}$	amount of reference resource produced in mode m of process i in time period t of season h
Q_{jht}	inventory level for resource j at time period t of season h
S_{jht}	amount of resource j discharged from the network in time period t of season h
TC	total annualized cost
V_i	capital cost for process i
λ_{il}	coefficient for segment l in piecewise-linear approximation for process i

Binary variables

w_{il}	equals 1 if the chosen capacity for process i is in the range of line segment l
x_i	equals 1 if process i is selected
$\bar{x}_j$	equals 1 if a storage facility is built for resource j
y_{imht}	equals 1 if process i operates in mode m in time period t of season h
$z_{imm'ht}$	equals 1 if operation of process i switched from mode m to mode m' at time t of season h

References

Bioenarea, 2016. The Bioenergy System Planners Handbook.
URL http://bisyplan.bioenarea.eu/html-files-en/02-02.html

CENER, 2017. GlobalWind herramienta de análisis del potencial eólico.
URL http://www.globalwindmap.com/VisorCENER/mapviewer.jsf;jsessionid=E9D845A6323D1366E931DE9462C27751

CORES, 2016. Consumos de gasolinas, gasóleos y fuelóleos por provincias y comunidades autónomas.
URL www.cores.es

Datosclima.es, 2017. Base de datos Meteorológica.
URL https://datosclima.es/Aemethistorico/Vientostad.php

Davis, W., Martín, M., 2014. Optimal year-round operation for methane production from CO2 and water using wind energy. Energy 69, 497–505.

Dommel, H., Tinney, W., 1968. Optimal Power Flow Solutions. IEEE Transactions on Power Apparatus and Systems PAS-87 (10), 1866–1876.

Dowling, A. W., Kumar, R., Zavala, V. M., 2017. A multi-scale optimization framework for electricity market participation. Applied Energy 190, 147–164.

Edwards, R. A. H., Šúri, M., Huld, T. A., Dallemand, J. F., 2006. GIS-Based Assessment of Cereal Straw Energy Resource in the European Union. Tech. rep., European Commission, Joint Research Centre Institute for Environment and Sustainability, Ispra.

Halamay, D. A., Brekken, T. K. A., Simmons, A., McArthur, S., 2011. Reserve requirement impacts of large-scale integration of wind, solar, and ocean wave power generation. IEEE Transactions on Sustainable Energy 2 (3), 321–328.

Heide, D., von Bremen, L., Greiner, M., Hoffmann, C., Speckmann, M., Bofinger, S., 2010. Seasonal optimal mix of wind and solar power in a future, highly renewable Europe. Renewable Energy 35 (11), 2483–2489.

Lara, C. L., Mallapragada, D., Papageorgiou, D. J., Venkatesh, A., Grossmann, I. E., 2017. Electric Power Infrastructure Planning: Mixed-Integer Programming Model and Nested Decomposition Algorithm. Under review, available on Optimization Online.

Lubin, M., Dunning, I., 2015. Computing in Operations Research Using Julia. INFORMS Journal on Computing 27 (2), 238–248.

MAPAMA, 2016. Encuestas Ganaderas, análisis del número de animales por tipos.
URL http://www.mapama.gob.es/es/estadistica/temas/estadisticas-agrarias/ganaderia/encuestas-ganaderas/

Marechal, F., Kalitventzeff, B., 2003. Targeting the integration of multi-period utility systems for site scale process integration. Applied Thermal Engineering 23 (14), 1763–1784.

Martín, M., 2016a. Methodology for solar and wind energy chemical storage facilities design under uncertainty: Methanol production from CO2 and hydrogen. Computers and Chemical Engineering 92, 43–54.

Martín, M., 2016b. Optimal year-round production of DME from CO2 and water using renewable energy. Journal of CO2 Utilization 13, 105–113.

Martín, M., Davis, W., 2016. Integration of wind, solar and biomass over a year for the constant production of CH4 from CO2 and water. Computers and Chemical Engineering 84, 313–325.

Martín, M., Grossmann, I. E., 2013. On the Systematic Synthesis of Sustainable Biorefineries. Industrial & Engineering Chemistry Research 52, 3044–3064.

Martín, M., Grossmann, I. E., 2017a. Optimal integration of a self sustained algae based facility with solar and/or wind energy. Journal of Cleaner Production 145, 336–347.

Martín, M., Grossmann, I. E., 2017b. Optimal integration of renewable based processes for fuels and power production: Spain case study. Applied Energy.

Mitra, S., Pinto, J. M., Grossmann, I. E., 2014. Optimal multi-scale capacity planning for power-intensive continuous processes under time-sensitive electricity prices and demand uncertainty. Part I: Modeling. Computers & Chemical Engineering 65, 89–101.

Padhy, N., 2004. Unit CommitmentA Bibliographical Survey. IEEE Transactions on Power Systems 19 (2), 1196–1205.

Red Electrica de Espana, 2017. Electricity Demand Data.
URL https://www.esios.ree.es/es/analisis/1293

SAIH Hidrosur, 2017. Datos a la carta.
URL http://www.redhidrosurmedioambiente.es/saih/datos/a/la/carta

Samsatli, S., Samsatli, N. J., 2015. A general spatio-temporal model of energy systems with a detailed account of transport and storage. Computers and Chemical Engineering 80, 155–176.

Sharifzadeh, M., Lubiano-walochik, H., Shah, N., 2017. Integrated renewable electricity generation considering uncertainties : The UK roadmap to 50 % power generation from wind and solar energies. Renewable and Sustainable Energy Reviews 72 (October 2016), 385–398.

Varbanov, P. S., Klemeš, J. J., 2011. Integration and management of renewables into Total Sites with variable supply and demand. Computers and Chemical Engineering 35 (9), 1815–1826.

Wassick, J. M., 2009. Enterprise-wide optimization in an integrated chemical complex. Computers & Chemical Engineering 33 (12), 1950–1963.

Yuan, Z., Chen, B., 2012. Process Synthesis for Addressing the Sustainable Energy Systems and Environmental Issues. AIChE Journal 58 (11), 3370–3389.

Yue, D., You, F., Snyder, S. W., 2014. Biomass-to-bioenergy and biofuel supply chain optimization: Overview, key issues and challenges. Computers and Chemical Engineering 66, 36–56.

Zhang, Q., Bremen, A. M., Grossmann, I. E., Sundaramoorthy, A., Pinto, J. M., 2018. Long-term electricity procurement for large industrial consumers under uncertainty. Industrial & Engineering Chemistry Research.

Zhang, Q., Grossmann, I. E., 2016. Enterprise-wide optimization for industrial demand side management: Fundamentals, advances, and perspectives. Chemical Engineering Research and Design 116, 114–131.

Zhang, Q., Sundaramoorthy, A., Grossmann, I. E., Pinto, J. M., 2016. A discrete-time scheduling model for continuous power-intensive process networks with various power contracts. Computers & Chemical Engineering 84, 382–393.

Zhang, Q., Sundaramoorthy, A., Grossmann, I. E., Pinto, J. M., 2017. Multiscale production routing in multicommodity supply chains with complex production facilities. Computers & Operations Research 79, 207–222.